

~~CONFIDENTIAL~~

Copy

5

RM A55H04a

NACA RM A55H04a

UNCLASSIFIED



# RESEARCH MEMORANDUM

EFFECT OF LEADING-EDGE SWEEPBACK ON LIFT, DRAG, AND  
PITCHING-MOMENT CHARACTERISTICS OF THIN WINGS  
OF ASPECT RATIO 3 AND TAPER RATIO 0.4 AT  
SUBSONIC AND SUPERSONIC SPEEDS

By Benton E. Wetzel

Ames Aeronautical Laboratory  
Moffett Field, Calif.

CLASSIFICATION CHANGED

UNCLASSIFIED

LIBRARY COPY

To

NOV 22 1955

By authority of

*NASA PA-1*

Date

*9-17-55*

LANGLEY AERONAUTICAL LABORATORY  
LIBRARY, NACA  
LANGLEY FIELD, VIRGINIA

CLASSIFIED DOCUMENT

This material contains information affecting the National Defense of the United States within the meaning of the espionage laws, Title 18, U.S.C., Secs. 793 and 794, the transmission or revelation of which in any manner to an unauthorized person is prohibited by law.

## NATIONAL ADVISORY COMMITTEE FOR AERONAUTICS

WASHINGTON

November 18, 1955

~~CONFIDENTIAL~~

UNCLASSIFIED



## NATIONAL ADVISORY COMMITTEE FOR AERONAUTICS

RESEARCH MEMORANDUM

EFFECT OF LEADING-EDGE SWEEPBACK ON LIFT, DRAG, AND

PITCHING-MOMENT CHARACTERISTICS OF THIN WINGS

OF ASPECT RATIO 3 AND TAPER RATIO 0.4 AT

SUBSONIC AND SUPERSONIC SPEEDS

By Benton E. Wetzel


## SUMMARY

Wind-tunnel studies were conducted to determine the effect of leading-edge sweepback on the lift, drag, and pitching-moment characteristics of 3-percent-thick wings of aspect ratio 3 and taper ratio 0.4. Data for a wing with  $45.0^\circ$  sweepback, tested in combination with a high-fineness-ratio body, are presented for angles of attack from  $-6^\circ$  to  $+17^\circ$  at Mach numbers from 0.61 to 0.93 and 1.20 to 1.90 at Reynolds numbers of 2.5 and 3.8 million. Comparisons are made between these data and the results for wings with  $19.1^\circ$  and  $53.1^\circ$  sweepback reported in NACA RM's A53A30 and A54J20, respectively.

Increasing the leading-edge sweepback of the wings decreased both the lift-curve slope and the variation of static longitudinal stability at zero lift with Mach number. In general, the drag coefficient at zero lift was decreased with increasing sweepback at supersonic speeds.

## INTRODUCTION

As part of a program devoted to the investigation of low-aspect-ratio wings, studies have been made in the Ames 6- by 6-foot supersonic wind tunnel to determine the effect of various amounts of leading-edge sweepback on the lift, drag, and pitching moment of thin wings of aspect ratio 3 and taper ratio 0.4. This paper presents the results of tests of a wing with  $45.0^\circ$  sweepback and compares these results with those for an unswept wing and for a wing with  $53.1^\circ$  sweepback, published previously in references 1 and 2, respectively. Similar studies have been made in the Ames 2- by 2-foot transonic wind tunnel and have been reported in reference 3.



## NOTATION

A	aspect ratio
b	wing span
c	local wing chord
$\bar{c}$	mean aerodynamic chord, $\frac{\int_0^{b/2} c^2 dy}{\int_0^{b/2} c dy}$
$C_D$	drag coefficient, $\frac{\text{drag}}{qS}$
$C_L$	lift coefficient, $\frac{\text{lift}}{qS}$
$C_m$	pitching-moment coefficient measured about the quarter point of the mean aerodynamic chord, $\frac{\text{pitching moment}}{qS\bar{c}}$
$\left(\frac{L}{D}\right)_{\max}$	maximum lift-drag ratio
M	free-stream Mach number
q	free-stream dynamic pressure
R	Reynolds number based on the mean aerodynamic chord
S	wing area, including area formed by extending the leading and trailing edges to the plane of symmetry
y	distance perpendicular to the plane of symmetry
$\frac{dC_L}{d\alpha}$	slope of lift curve at zero lift, per deg
$\frac{dC_m}{dC_L}$	slope of pitching-moment curve at zero lift
$\alpha$	angle of attack of body axis, deg
$\Lambda$	angle of leading-edge sweepback, deg

## APPARATUS AND MODEL

The investigation was performed in the Ames 6- by 6-foot supersonic wind tunnel. This wind tunnel, which is of a closed-section, variable-pressure type, is described in reference 4. It can be operated at Mach numbers varying from 0.60 to that for "choking" and from 1.20 to 1.90. Model wing-body combinations are sting-mounted in the wind tunnel, and the aerodynamic forces and moments are measured with an internal electrical strain-gage balance.

The model for the present tests utilized a 3-percent-thick wing of aspect ratio 3 and taper ratio 0.4. Leading-edge sweepback was  $45.0^\circ$ . A dimensional sketch of this model, together with sketches of the other models used in studying the effect of sweepback, is shown in figure 1. The profile used was biconvex with an elliptical nose. Coordinates of the airfoil are presented in table I. The wing was constructed of steel and was tested in combination with a Sears-Haack body. The equation of that body is included in figure 1.

## TESTS AND PROCEDURES

For the wing-body combination employing the wing with  $45.0^\circ$  sweepback, lift, drag, and pitching moment were measured throughout an angle-of-attack range from  $-6^\circ$  to a maximum of  $+17^\circ$  at Mach numbers of 0.61 to 0.93 and 1.20 to 1.90. Data were obtained at Reynolds numbers of 2.5 and 3.8 million, based on the mean aerodynamic chord of the wing. Because of wind-tunnel power limitations, the maximum Mach number of the tests at the higher Reynolds number was 1.60.

## REDUCTION OF DATA

Data presented in this report have been reduced to NACA coefficient form. The data have been corrected to account for the differences known to exist between measurements made in the wind tunnel and in a free-air stream. The corrections, which were applied in accordance with the procedures used in reference 5, account for the following factors:

1. The change in Mach number at subsonic speeds resulting from the constriction of the flow by the wind-tunnel walls.
2. The induced effects of the wind-tunnel walls at subsonic speeds resulting from lift on the model.

3. The inclination of the air stream in the wind tunnel. This correction was of the order of  $-0.13^\circ$  and  $-0.10^\circ$  at subsonic and supersonic speeds, respectively. Although sufficient data were not available to permit the application of such a correction to the data for the unswept wing of reference 1, the stream inclination for that model should be of the same order as for the present model. Thus, at a lift coefficient of 0.5 the correction to the drag coefficient would be about  $-0.0010$ .

4. The effect on the drag measurements due to the longitudinal variation of static pressure in the test section.

5. The effect of support interference on the pressure at the base of the model. The base pressure was measured and the drag was adjusted to correspond to that drag for which the base pressure would be equal to the free-stream pressure.

## RESULTS AND DISCUSSION

Results obtained for three wing-body combinations, having taper ratio of 0.4 and thickness-chord ratio of 0.03, have been used to study the effect of leading-edge sweepback on lift, drag, and pitching moment. The geometric variables of the wings, sketches of which are presented in figure 1, are tabulated below.

Wing	$\Lambda$ , deg	A	Profile
Unswept	19.1	3.1	Biconvex with elliptical nose
Swept	45.0	3.0	Biconvex with elliptical nose
Swept	53.1	3.0	NACA 0003-63

Although two different airfoils were utilized, the differences were small, as shown in figure 2. It is believed that these differences did not obscure the effect of a variation of leading-edge sweepback.

Lift, drag, and pitching-moment data for the wing with  $45.0^\circ$  sweepback of the leading edge are presented in table II for all test conditions. Similarly tabulated data for the unswept wing and the wing with  $53.1^\circ$  sweepback can be found in references 1 and 2, respectively. A portion of the basic data for the wing with  $45.0^\circ$  sweepback is shown in figure 3. An increase in Reynolds number from 2.5 to 3.8 million had no significant effect on the lift, drag, or pitching-moment characteristics.

The effect of leading-edge sweepback will be illustrated with results for the highest Reynolds numbers at which data could be obtained throughout the entire range of Mach numbers.

### Lift

The effect of sweepback on the variation of the lift-curve slope at zero lift with Mach number is shown in figure 4. Increasing the angle of sweepback resulted in a reduction of the experimental lift-curve slopes at subsonic and supersonic speeds. The theoretical slopes for the wing alone were obtained from references 6, 7, and 8; wing-body interference was accounted for by the method of reference 9. The variation of lift coefficient with angle of attack is presented in figure 5 for the three wings. At a Mach number of 0.6 an increase in maximum lift coefficient with increasing sweepback is clearly indicated.

### Pitching Moment

The effect of sweepback on the variation of the static longitudinal stability derivative  $dC_m/dC_L$ , measured at zero lift, with Mach number is shown in figure 6. Increasing the sweepback decreased the over-all center-of-lift travel with Mach number. This effect was shown to be most significant when sweepback was increased from  $19.1^\circ$  to  $45.0^\circ$ .

All of the wings had nonlinear variations of pitching-moment coefficient with lift coefficient at subsonic speeds, as illustrated in figure 7. In the Mach number range from 0.60 to 0.91 abrupt changes in the pitching-moment coefficient generally occurred for the models with  $19.1^\circ$  and  $53.1^\circ$  sweepback at lift coefficients well below the maximum lift coefficient. For the wing with  $45.0^\circ$  sweepback, however, more moderate changes occurred below a lift coefficient of 0.8 at Mach numbers of 0.61 and 0.81. It is interesting to note that the lift coefficient at which the pitching-moment coefficient of the wing with  $19.1^\circ$  sweepback increased abruptly was greatly reduced when Mach number was increased from 0.81 to 0.91.

### Drag

The effect of sweepback on the variation of drag coefficient with Mach number is presented in figure 8 for several lift coefficients. In general, as sweepback was increased, the drag coefficients increased at subsonic speeds and decreased at supersonic speeds. The effect of sweepback on the drag coefficient at zero lift, however, was small at subsonic speeds.

Comparison of the drag coefficients at lift coefficients other than zero with those at zero lift shows that, when sweepback was increased, the drag due to lift was increased at subsonic speeds. An increase in sweepback from  $19.1^\circ$  to  $45.0^\circ$  resulted in a smaller increase in drag due to

lift than did an increase in sweepback from  $45.0^\circ$  to  $53.1^\circ$ , except at the higher lift coefficients at Mach numbers greater than 0.7. At supersonic speeds an increase in sweepback from  $19.1^\circ$  to  $45.0^\circ$  reduced the drag due to lift, while an increase from  $45.0^\circ$  to  $53.1^\circ$  resulted in an increase in drag due to lift. Thus, sweepback of the order of  $45.0^\circ$  provided a large portion of the benefits of sweepback at supersonic speeds without large penalties at subsonic speeds.

The maximum lift-drag ratio and range parameter  $M(L/D)_{\max}$  are presented as a function of Mach number in figure 9. Increasing sweepback decreased the maximum lift-drag ratios at Mach numbers from 0.60 to 0.85 and increased them at Mach numbers from 1.20 to 1.90, as shown in figure 9(a). The gain in range obtained at supersonic speeds as a result of increased sweepback is illustrated in figure 9(b).

Although the effects of leading-edge sweepback on lift and pitching moment shown herein are similar to those reported in reference 3, differences will be noted between the effects of sweepback on the drag characteristics as shown in the two papers. This results primarily from a difference in the minimum drag coefficients of the unswept wings of the two investigations. The unswept wing used in the investigation reported in reference 3 had a biconvex airfoil, while the unswept wing of the present tests had a biconvex airfoil with an elliptical nose section. Studies devoted to changes in profile (ref. 1) have shown that, for the unswept wing, addition of an elliptical nose section to the biconvex airfoil results in a reduction of the minimum drag coefficient at subsonic Mach numbers and an increase at Mach numbers greater than 1.2. Therefore, in order to minimize the effect of profile differences, data for the unswept wing having a biconvex airfoil with an elliptical nose section (ref. 1) were used in the present study.

#### CONCLUDING REMARKS

Wind-tunnel studies of three wings of aspect ratio 3 and taper ratio 0.4 showed that an increase in leading-edge sweepback had the following effects on the lift, drag, and pitching-moment characteristics:

1. Lift-curve slope at zero lift was decreased at both subsonic and supersonic speeds. Results at a Mach number of 0.6 indicated a substantial increase in the maximum lift coefficient.
2. The variation of static longitudinal stability (at zero lift) with Mach number was decreased.
3. The drag coefficient at zero lift was, in general, reduced at supersonic speeds. The maximum lift-drag ratios were decreased at Mach numbers from 0.60 to 0.85 and increased at Mach numbers from 1.20 to 1.90.

Results presented for the wing with  $45.0^\circ$  sweepback showed that an increase in Reynolds number from 2.5 to 3.8 million had no significant effect on the lift, drag, or pitching-moment characteristics.

Ames Aeronautical Laboratory  
National Advisory Committee for Aeronautics  
Moffett Field, Calif., Aug. 4, 1955

#### REFERENCES

1. Hall, Charles F.: Lift, Drag, and Pitching Moment of Low-Aspect-Ratio Wings at Subsonic and Supersonic Speeds. NACA RM A53A30, 1953.
2. Wetzel, Benton E.: Effect of Taper Ratio on Lift, Drag, and Pitching-Moment Characteristics of Thin Wings of Aspect Ratio 3 With  $53.1^\circ$  Sweepback of Leading Edge at Subsonic and Supersonic Speeds. NACA RM A54J20, 1955.
3. Knechtel, Earl D., and Summers, James L.: Effects of Sweep and Taper Ratio on the Longitudinal Characteristics of an Aspect Ratio 3 Wing-Body Combination at Mach Numbers from 0.6 to 1.4. NACA RM A55A03, 1955.
4. Frick, Charles W., and Olson, Robert N.: Flow Studies in the Asymmetric Nozzle of the Ames 6- by 6-Foot Supersonic Wind Tunnel. NACA RM A9E24, 1949.
5. Boyd, John W.: Aerodynamic Characteristics of Two 25-Percent Trailing-Edge Flaps on an Aspect Ratio 2 Triangular Wing at Subsonic and Supersonic Speeds. NACA RM A52D01c, 1952.
6. DeYoung, John, and Harper, Charles W.: Theoretical Symmetric Span Loading at Subsonic Speeds for Wings Having Arbitrary Plan Form. NACA Rep. 921, 1948.
7. Jones, Robert T.: Properties of Low-Aspect-Ratio Pointed Wings at Speeds Below and Above the Speed of Sound. NACA Rep. 835, 1946. (Formerly NACA TN 1032)
8. Lapin, Ellis: Charts for the Computation of Lift and Drag of Finite Wings at Supersonic Speeds. Rep. SM-13480, Douglas Aircraft Co., Santa Monica, Oct. 14, 1949.
9. Nielsen, Jack N., Kaattari, George E., and Anastasio, Robert F.: A Method for Calculating the Lift and Center of Pressure of Wing-Body-Tail Combinations at Subsonic, Transonic, and Supersonic Speeds. NACA RM A53G08, 1953.



TABLE I.- COORDINATES OF BICONVEX AIRFOIL WITH ELLIPTICAL NOSE SECTION  
[All coordinates for sections parallel to the plane of symmetry]

Station, percent c	Ordinate, percent c
0	0
.75	.259
1.25	.333
2.50	.468
5.00	.653
7.50	.790
10.00	.900
15	1.071
20	1.200
25	1.300
30	1.375
40	1.469
50	1.500
60	1.440
70	1.260
80	.960
85	.765
90	.540
95	.285
100	0
L.E. radius: 0.045 percent c	

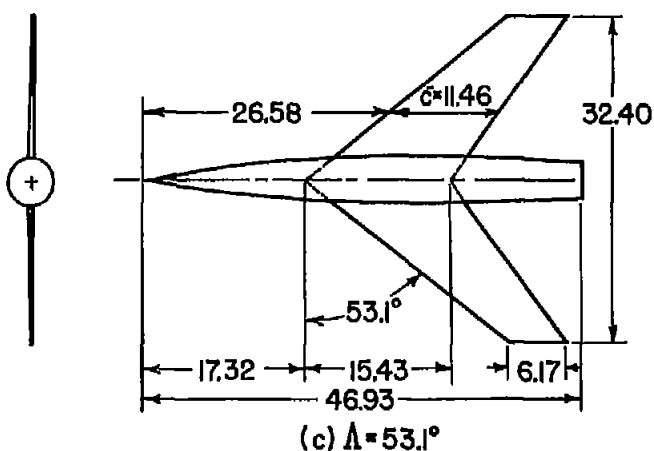
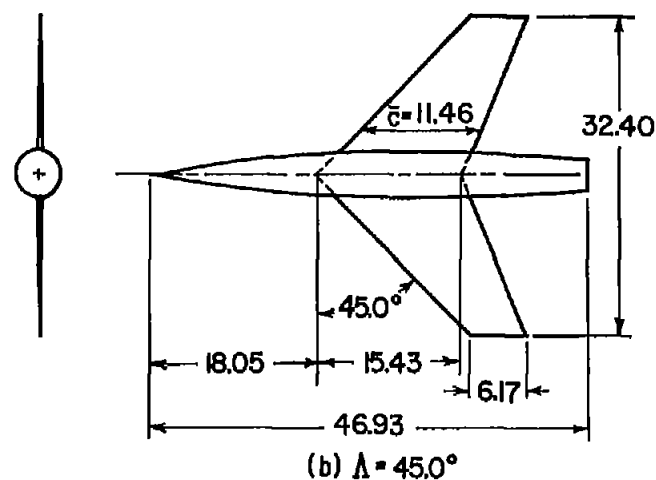
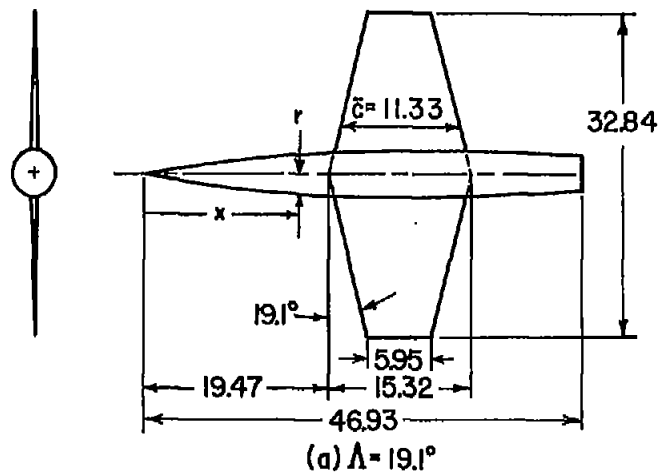
TABLE II.- AERODYNAMIC CHARACTERISTICS OF 45.0° SWEEP WING OF ASPECT RATIO 3 AND TAPER RATIO 0.4 HAVING A 3-PERCENT-THICK BICONVEX AIRFOIL WITH ELLIPTICAL NOSE SECTION

(a) R = 2.5 million

M	$\alpha$	$C_L$	$C_D$	$C_m$	M	$\alpha$	$C_L$	$C_D$	$C_m$	M	$\alpha$	$C_L$	$C_D$	$C_m$	M	$\alpha$	$C_L$	$C_D$	$C_m$
0.61	-5.98	-0.365	0.0397	0.013	0.93	-5.79	-0.487	0.0549	0.065	1.40	-5.36	-0.322	0.0437	0.071	1.70	-5.31	-0.256	0.0381	0.075
	-4.49	-0.287	0.0274	0.008		-4.66	-0.388	0.0372	0.044		-4.38	-0.260	0.0339	0.056		-4.26	-0.208	0.0300	0.044
	-3.40	-0.208	0.0182	0.004		-3.73	-0.284	0.0236	0.026		-3.26	-0.195	0.0231	0.040		-3.22	-0.157	0.0231	0.033
	-2.32	-0.137	0.0120	0.003		-2.40	-0.180	0.0145	0.011		-2.20	-0.133	0.0187	0.025		-2.18	-0.107	0.0182	0.022
	-1.23	-0.072	0.0090	0.001		-1.28	-0.088	0.0096	0.001		-1.15	-0.069	0.0148	0.012		-1.13	-0.055	0.0150	0.011
	-0.69	-0.040	0.0077	0		-0.71	-0.046	0.0082	0.001		-0.61	-0.039	0.0140	0.006		-0.60	-0.030	0.0140	0.006
	-0.42	-0.026	0.0073	0		-0.43	-0.026	0.0077	0.002		-0.38	-0.023	0.0136	0.003		-0.33	-0.017	0.0137	0.003
	0.08	0.002	0.0072	-0.001		0.08	0.003	0.0077	-0.001		0.11	0.003	0.0137	-0.002		0.11	0.004	0.0138	-0.002
	0.40	0.020	0.0072	-0.001		0.42	0.030	0.0077	-0.001		0.39	0.021	0.0140	-0.005		0.38	0.019	0.0138	-0.005
	0.94	0.049	0.0084	0		0.96	0.068	0.0091	-0.002		0.92	0.052	0.0146	-0.011		0.91	0.045	0.0143	-0.010
	2.03	0.118	0.0106	-0.002		2.12	0.164	0.0131	-0.013		1.99	0.118	0.0176	-0.024		1.97	0.098	0.0169	-0.022
	3.12	0.192	0.0158	-0.005		3.24	0.263	0.0206	-0.027		3.04	0.182	0.0230	-0.036		3.02	0.149	0.0211	-0.033
	4.21	0.268	0.0234	-0.009		4.37	0.364	0.0323	-0.043		4.10	0.246	0.0304	-0.054		4.06	0.200	0.0273	-0.044
	5.30	0.349	0.0345	-0.014							5.15	0.311	0.0397	-0.069		5.10	0.249	0.0350	-0.055
	6.40	0.435	0.0494	-0.018							6.20	0.374	0.0510	-0.085		6.14	0.298	0.0444	-0.066
	8.55	0.560	0.0837	-0.016							8.31	0.499	0.0809	-0.115		8.23	0.397	0.0680	-0.088
	10.67	0.667	0.1248	-0.015							10.41	0.614	0.1179	-0.142		10.31	0.493	0.0982	-0.109
	12.79	0.762	0.1719	-0.019							12.50	0.717	0.1615	-0.163		12.39	0.579	0.1355	-0.129
	14.88	0.838	0.2214	-0.024							13.59	0.768	0.1866	-0.174		13.47	0.664	0.1749	-0.147
	16.90	0.862	0.2634	-0.045												16.75	0.744	0.2221	-0.162
	17.90	0.871	0.2854	-0.057															
0.81	-5.69	-0.412	0.0493	0.023	1.20	-5.40	-0.398	0.0481	0.081	1.50	-5.34	-0.296	0.0412	0.065	1.90	-5.34	-0.226	0.0361	0.048
	-4.58	-0.324	0.0302	0.015		-4.33	-0.316	0.0355	0.061		-4.29	-0.240	0.0318	0.052		-4.29	-0.185	0.0287	0.039
	-3.46	-0.234	0.0200	0.008		-3.22	-0.235	0.0257	0.044		-3.24	-0.180	0.0240	0.038		-3.23	-0.140	0.0228	0.029
	-2.36	-0.154	0.0132	0.004		-2.21	-0.158	0.0191	0.029		-2.20	-0.122	0.0181	0.025		-2.18	-0.095	0.0185	0.020
	-1.25	-0.077	0.0094	0		-1.15	-0.083	0.0144	0.014		-1.14	-0.063	0.0146	0.011		-1.12	-0.049	0.0150	0.010
	-0.70	-0.042	0.0077	0		-0.38	-0.028	0.0123	0.004		-0.60	-0.034	0.0138	0.006		-0.59	-0.027	0.0155	0.005
	-0.42	-0.026	0.0073	-0.001		-0.65	-0.046	0.0127	0.007		-0.33	-0.019	0.0136	0.003		-0.33	-0.016	0.0155	0.003
	0.08	0.001	0.0073	-0.001		0.11	0.001	0.0125	-0.001		0.11	0.004	0.0136	-0.002		0.11	0.003	0.0151	-0.001
	0.41	0.026	0.0073	-0.001		0.39	0.023	0.0129	-0.004		0.39	0.021	0.0137	-0.005		0.42	0.016	0.0152	-0.004
	0.95	0.056	0.0087	0		0.93	0.060	0.0139	-0.011		0.92	0.049	0.0141	-0.010		0.91	0.039	0.0156	-0.009
	2.07	0.135	0.0116	-0.005		2.00	0.136	0.0177	-0.025		1.98	0.111	0.0169	-0.023		1.96	0.087	0.0179	-0.019
	3.18	0.219	0.0175	-0.010		3.06	0.214	0.0232	-0.040		3.03	0.171	0.0220	-0.037		3.00	0.132	0.0219	-0.029
	4.29	0.308	0.0268	-0.016		4.12	0.293	0.0315	-0.057		4.08	0.229	0.0290	-0.050		4.04	0.176	0.0272	-0.038
	5.41	0.397	0.0396	-0.024		5.18	0.376	0.0426	-0.077		5.13	0.286	0.0377	-0.064		5.08	0.220	0.0339	-0.048
	6.52	0.481	0.0558	-0.028		6.24	0.463	0.0572	-0.098		6.18	0.344	0.0484	-0.078		6.11	0.264	0.0423	-0.058
	8.67	0.601	0.0821	-0.031		8.37	0.638	0.0969	-0.139		8.28	0.460	0.0758	-0.105		8.19	0.351	0.0636	-0.077
	10.83	0.721	0.1382	-0.041		10.50	0.761	0.1441	-0.140		10.37	0.567	0.1100	-0.130		10.26	0.438	0.0909	-0.095
	12.92	0.788	0.1827	-0.041							12.46	0.665	0.1506	-0.153		12.34	0.517	0.1228	-0.112
	15.00	0.844	0.2303	-0.054							14.55	0.759	0.1975	-0.173		14.41	0.593	0.1605	-0.127
	17.05	0.891	0.2797	-0.072												16.48	0.667	0.2041	-0.140
	18.07	0.909	0.3052	-0.088												17.52	0.703	0.2279	-0.147
0.91	-5.77	-0.472	0.0525	0.048	1.30	-5.38	-0.350	0.0437	0.074	1.60	-5.33	-0.276	0.0403	0.060					
	-4.65	-0.373	0.0349	0.031		-4.32	-0.282	0.0346	0.057		-4.28	-0.223	0.0312	0.048					
	-3.51	-0.266	0.0219	0.016		-3.27	-0.210	0.0260	0.041		-3.23	-0.169	0.0238	0.035					
	-2.39	-0.171	0.0139	0.007		-2.21	-0.141	0.0200	0.026		-2.19	-0.114	0.0183	0.023					
	-1.27	-0.085	0.0097	0		-1.15	-0.075	0.0158	0.013		-1.14	-0.059	0.0147	0.011					
	-0.71	-0.046	0.0080	-0.001		-0.61	-0.041	0.0148	0.007		-0.60	-0.031	0.0137	0.006					
	-0.43	-0.027	0.0074	-0.001		-0.38	-0.024	0.0147	0.004		-0.33	-0.018	0.0133	0.003					
	0.08	0.003	0.0073	-0.001		0.11	0.002	0.0145	-0.001		0.11	0.003	0.0133	-0.001					
	0.42	0.029	0.0073	-0.002		0.39	0.023	0.0150	-0.005		0.38	0.019	0.0134	-0.005					
	0.97	0.064	0.0091	-0.001		0.93	0.056	0.0159	-0.011		0.92	0.047	0.0139	-0.010					
	2.10	0.153	0.0128	-0.008		1.99	0.126	0.0194	-0.025		1.98	0.103	0.0166	-0.022					
	3.23	0.247	0.0191	-0.017		3.05	0.196	0.0247	-0.040		3.03	0.159	0.0214	-0.035					
	4.37	0.362	0.0312	-0.037		4.11	0.266	0.0323	-0.055		4.07	0.214	0.0278	-0.047					
	5.50	0.466	0.0475	-0.056		5.17	0.336	0.0422	-0.072		5.12	0.266	0.0360	-0.059					
	6.70	0.542	0.0654	-0.063		6.22	0.406	0.0548	-0.089		6.16	0.320	0.0459	-0.071					
	8.87	0.672	0.1080	-0.075		8.33	0.441	0.0671	-0.121		8.26	0.427	0.0714	-0.096					
						10.44	0.665	0.1273	-0.149		10.34	0.526	0.1031	-0.119					
						12.53	0.773	0.1737	-0.171		12.43	0.621	0.1412	-0.141					
											14.51	0.710	0.1855	-0.161					
											15.15	0.738	0.2004	-0.166					

TABLE II.- AERODYNAMIC CHARACTERISTICS OF 45.0° SWEEP WING OF ASPECT RATIO 3 AND TAPER RATIO 0.4 HAVING A 3-PERCENT-THICK BICONVEX AIRFOIL WITH ELLIPTICAL NOSE SECTION - Concluded  
(b) R = 3.8 million

M	$\alpha$	$C_L$	$C_D$	$C_m$	M	$\alpha$	$C_L$	$C_D$	$C_m$	M	$\alpha$	$C_L$	$C_D$	$C_m$
0.61	-5.71	-0.362	0.0388	0.010	0.93	-6.01	-0.500	0.0558	0.064	1.40	-5.53	-0.326	0.0449	0.070
	-4.60	-.285	.0266	.006		-4.85	-.401	.0378	.045		-4.44	-.261	.0342	.055
	-3.48	-.214	.0179	.004		-3.67	-.288	.0234	.024		-3.35	-.194	.0258	.039
	-2.38	-.146	.0123	.002		-2.50	-.193	.0147	.013		-2.27	-.132	.0201	.026
	-1.28	-.078	.0097	0		-1.34	-.098	.0102	.005		-1.18	-.068	.0164	.013
	-.71	-.044	.0089	0		-.75	-.054	.0089	.002		-.63	-.038	.0154	.007
	-.43	-.028	.0088	0		-.46	-.032	.0086	0		-.35	-.021	.0151	.004
	.08	.001	.0087	0		.10	.009	.0086	-.002		.12	.006	.0150	-.002
	.41	.023	.0088	0		.45	.035	.0087	-.003		.41	.026	.0153	-.006
	.98	.057	.0094	-.001		1.04	.078	.0096	-.006		.97	.058	.0160	-.012
	2.09	.128	.0111	-.003		2.20	.170	.0128	-.013		2.06	.124	.0193	-.025
	3.20	.199	.0154	-.006		3.38	.277	.0201	-.028		3.14	.187	.0243	-.038
	4.31	.272	.0225	-.008		4.55	.378	.0315	-.042		4.23	.252	.0313	-.053
	5.43	.352	.0337	-.013							5.32	.318	.0406	-.068
	6.55	.430	.0491	-.017							6.40	.380	.0522	-.083
	8.77	.578	.0879	-.017							8.56	.501	.0819	-.111
	10.93	.676	.1283	-.015										
	13.08	.772	.1761	-.019										
	14.83	.836	.2181	-.023										
.81	-5.87	-.414	.0455	.021	1.20	-5.61	-.400	.0490	.080	1.50	-5.50	-.299	.0419	.064
	-4.73	-.327	.0305	.013		-4.51	-.320	.0363	.062		-4.42	-.241	.0324	.051
	-3.58	-.242	.0199	.008		-3.51	-.237	.0268	.044		-3.34	-.181	.0248	.037
	-2.44	-.163	.0133	.005		-2.30	-.158	.0197	.029		-2.16	-.123	.0194	.025
	-1.31	-.084	.0098	.002		-1.20	-.083	.0158	.015		-1.18	-.063	.0159	.012
	-.73	-.047	.0089	0		-.65	-.046	.0147	.009		-.63	-.033	.0150	.006
	-.45	-.029	.0088	0		-.36	-.026	.0144	.005		-.35	-.019	.0146	.003
	.09	.003	.0085	-.001		.16	.007	.0144	-.001		.12	.006	.0147	-.002
	.43	.028	.0087	-.001		.42	.029	.0145	-.005		.41	.023	.0149	-.005
	1.01	.064	.0094	-.002		.98	.067	.0154	-.012		.96	.054	.0155	-.011
	2.15	.146	.0119	-.006		2.08	.144	.0184	-.026		2.05	.116	.0184	-.024
	3.29	.228	.0172	-.010		3.18	.222	.0237	-.040		3.13	.175	.0233	-.037
	4.44	.312	.0258	-.015		4.29	.304	.0319	-.057		4.20	.233	.0301	-.050
	5.60	.407	.0401	-.024		5.39	.386	.0433	-.077		5.29	.294	.0391	-.064
	6.73	.488	.0575	-.029		6.50	.471	.0580	-.097		6.36	.352	.0498	-.077
	8.95	.605	.0945	-.028							8.51	.463	.0766	-.103
	10.26	.683	.1228	-.038										
.91	-6.02	-.495	.0544	.054	1.30	-5.60	-.354	.0467	.074	1.60	-5.60	-.280	.0410	.061
	-5.00	-.389	.0370	.032		-4.47	-.285	.0354	.057		-4.50	-.226	.0317	.048
	-3.66	-.277	.0220	.016		-3.38	-.211	.0265	.041		-3.39	-.171	.0242	.036
	-2.49	-.182	.0143	.009		-2.28	-.142	.0204	.027		-2.25	-.117	.0187	.024
	-1.33	-.094	.0101	.004		-1.19	-.074	.0167	.013		-1.17	-.061	.0152	.012
	-.75	-.052	.0088	.001		-.64	-.040	.0156	.007		-.62	-.033	.0144	.006
	-.45	-.032	.0086	0		-.35	-.022	.0153	.004		-.35	-.018	.0141	.004
	.09	.005	.0086	-.001		.12	.005	.0154	-.002		.12	.007	.0141	-.002
	.44	.031	.0087	-.002		.41	.028	.0155	-.006		.40	.023	.0141	-.005
	1.03	.072	.0096	-.004		.97	.062	.0163	-.012		.96	.051	.0147	-.011
	2.19	.165	.0129	-.011		2.07	.133	.0194	-.026		2.03	.108	.0177	-.023
	3.36	.260	.0192	-.018		3.16	.203	.0245	-.040		3.11	.162	.0225	-.035
	4.55	.373	.0305	-.035		4.25	.274	.0320	-.055		4.18	.217	.0291	-.047
	5.72	.478	.0482	-.058		5.35	.347	.0421	-.072		5.25	.272	.0373	-.059
	6.86	.560	.0689	-.070		6.44	.416	.0548	-.089		6.33	.328	.0477	-.072
						8.00	.510	.0770	-.111		8.46	.431	.0731	-.095
											9.84	.497	.0931	-.110



Equation for body radius:

$$r = r_0 \left[ 1 - \left( 1 - \frac{2x}{l} \right)^2 \right]^{\frac{3}{4}}$$

Maximum radius,  $r_0 = 2.38$

Length for closure,  $l = 59.50$

All dimensions in inches unless otherwise noted

Figure 1.- Dimensional sketches of models.

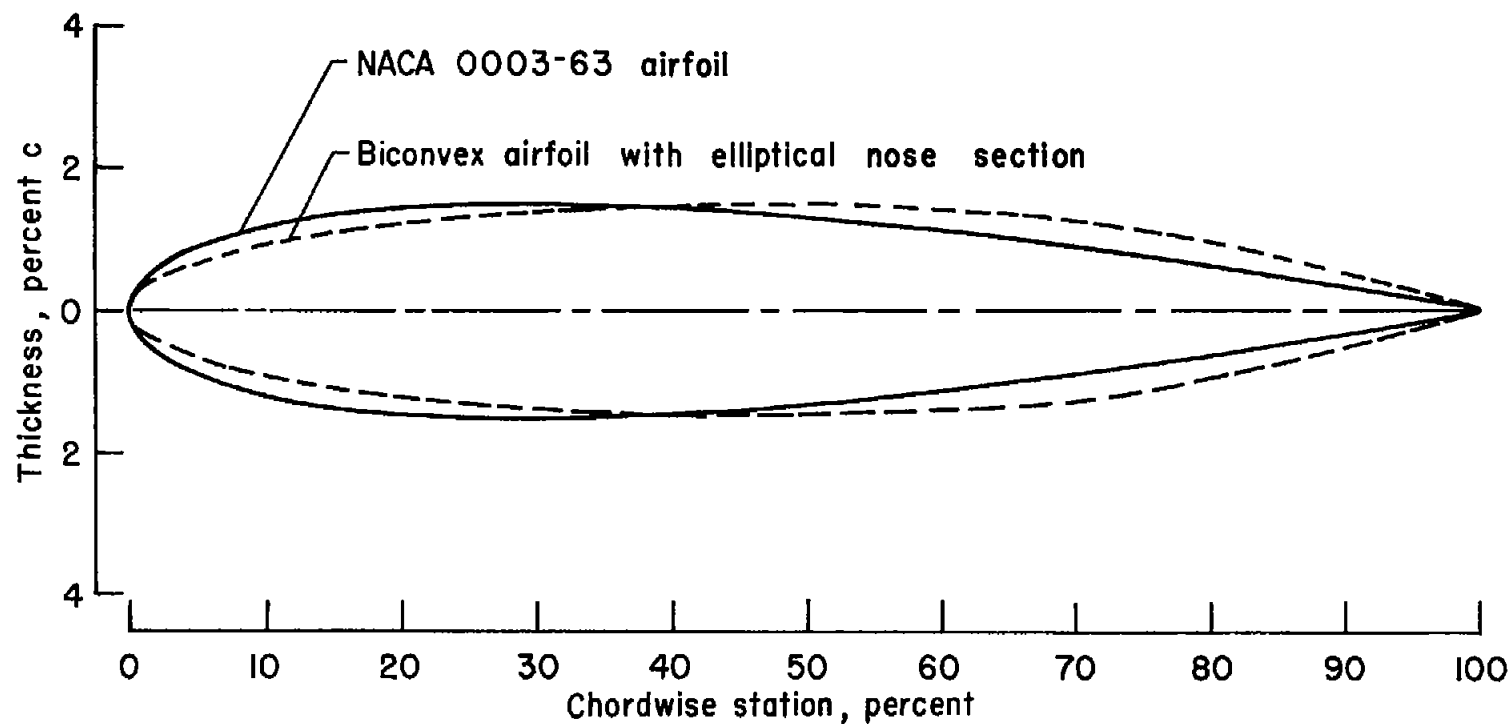
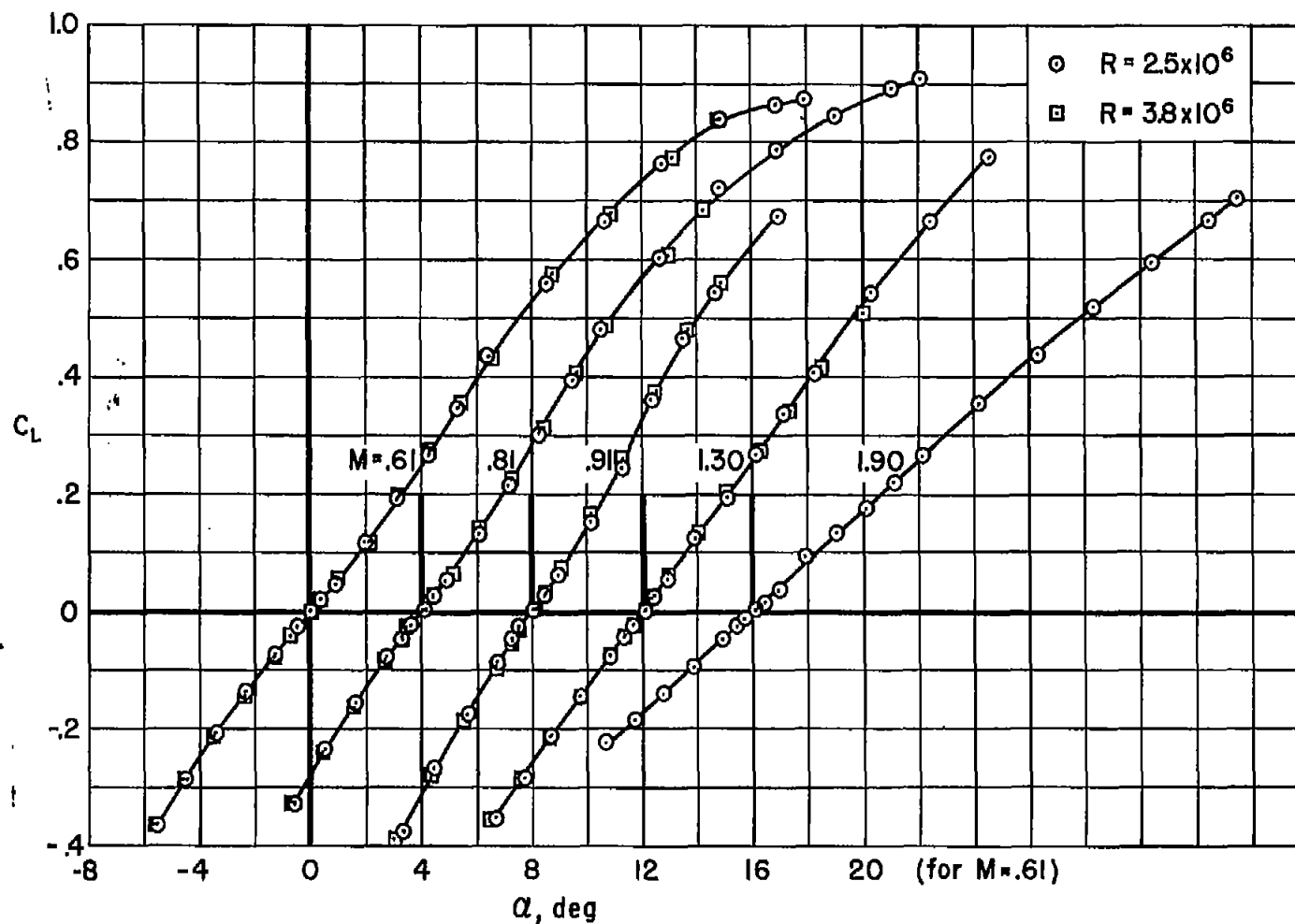


Figure 2.- Comparison of thickness distributions for an NACA 0003-63 airfoil and a biconvex airfoil with an elliptical nose section.



(a)  $C_L$  vs.  $\alpha$

Figure 3.- Aerodynamic characteristics of a wing-body combination employing a wing of aspect ratio 3 with  $45.0^\circ$  sweepback of the leading edge and a taper ratio 0.4.

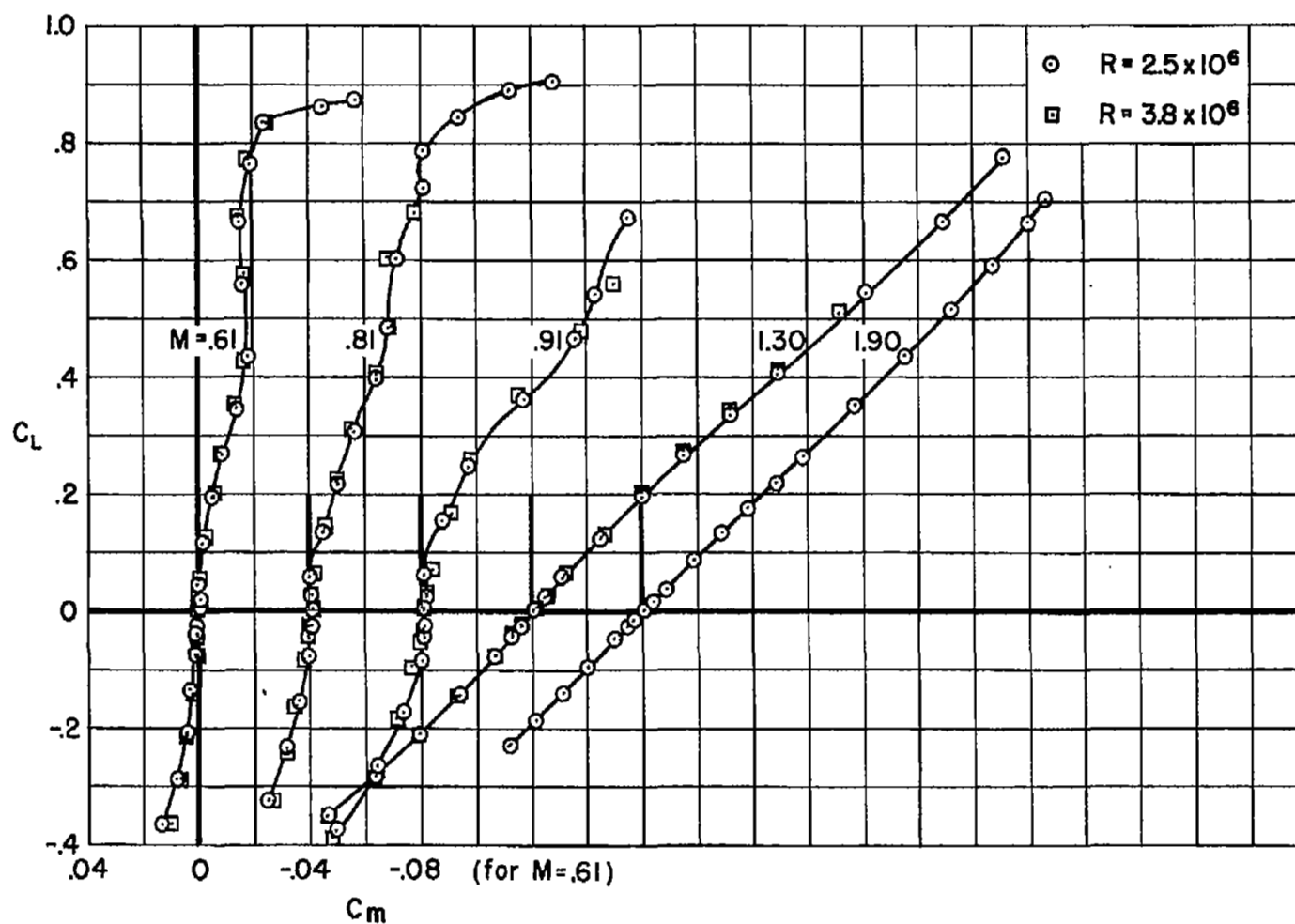
(b)  $C_L$  vs.  $C_m$ 

Figure 3.- Continued.

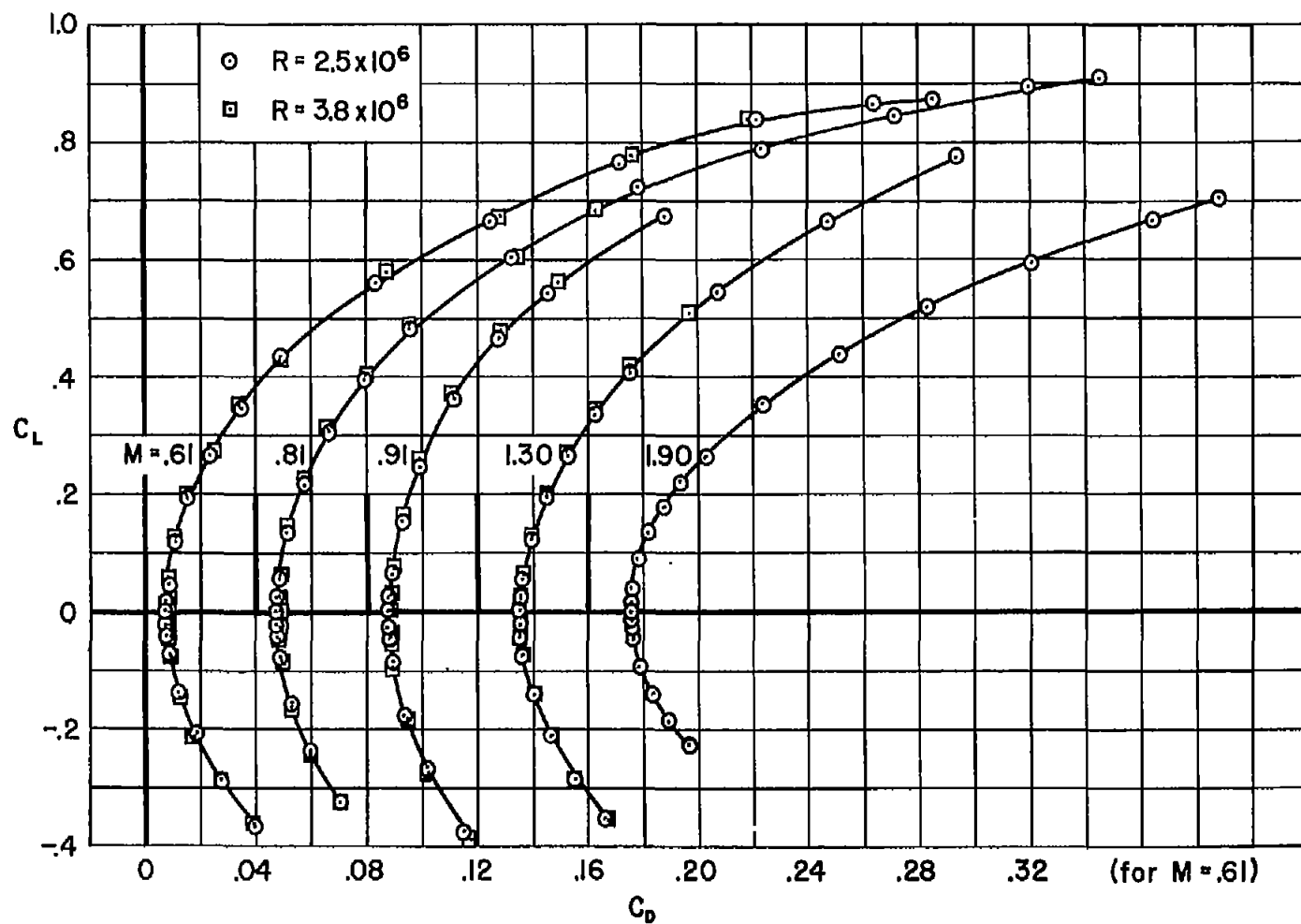
(c)  $C_L$  vs.  $C_D$ 

Figure 3.- Concluded.



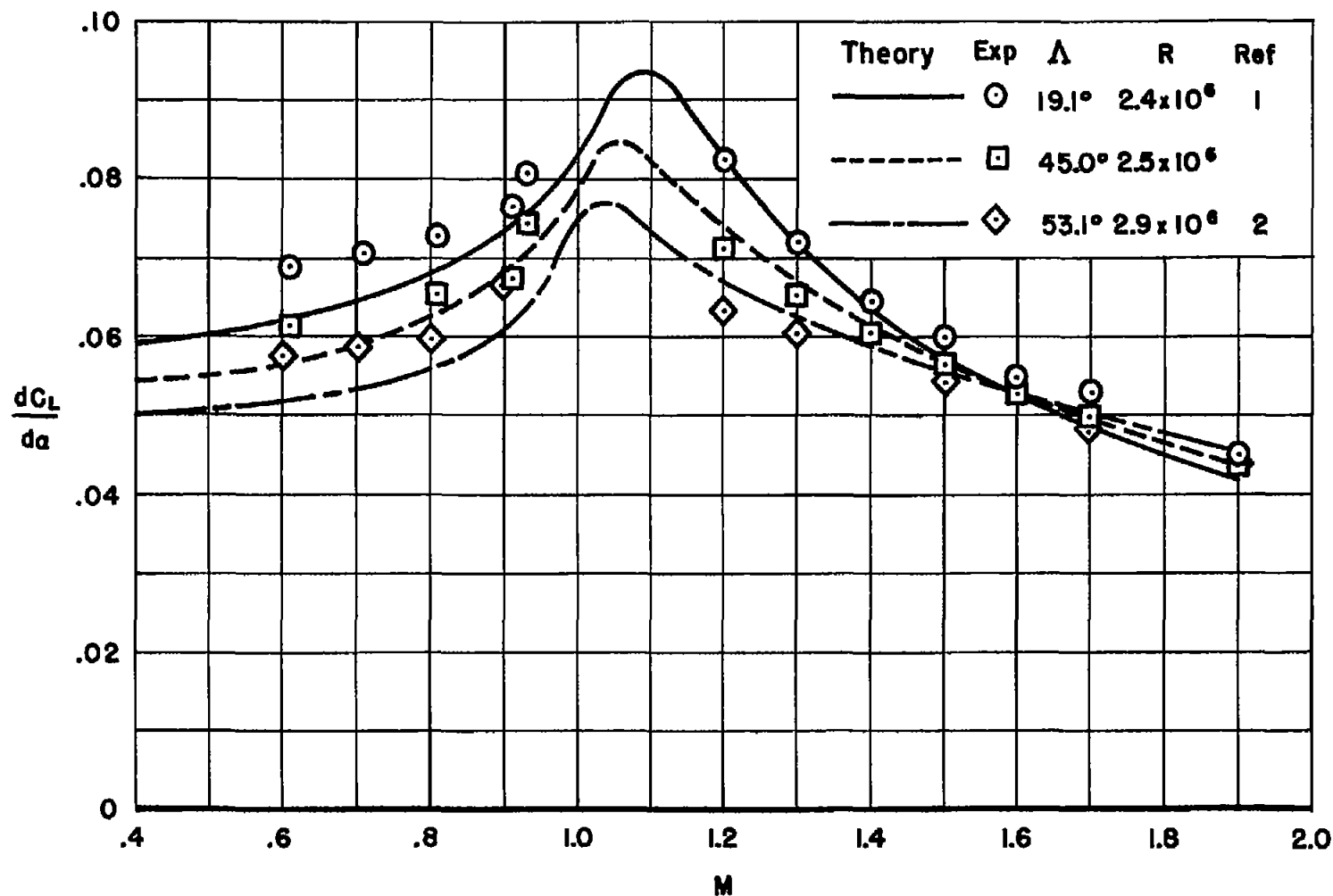


Figure 4.- Effect of leading-edge sweepback on the variation with Mach number of the theoretical and experimental lift-curve slopes at zero lift.

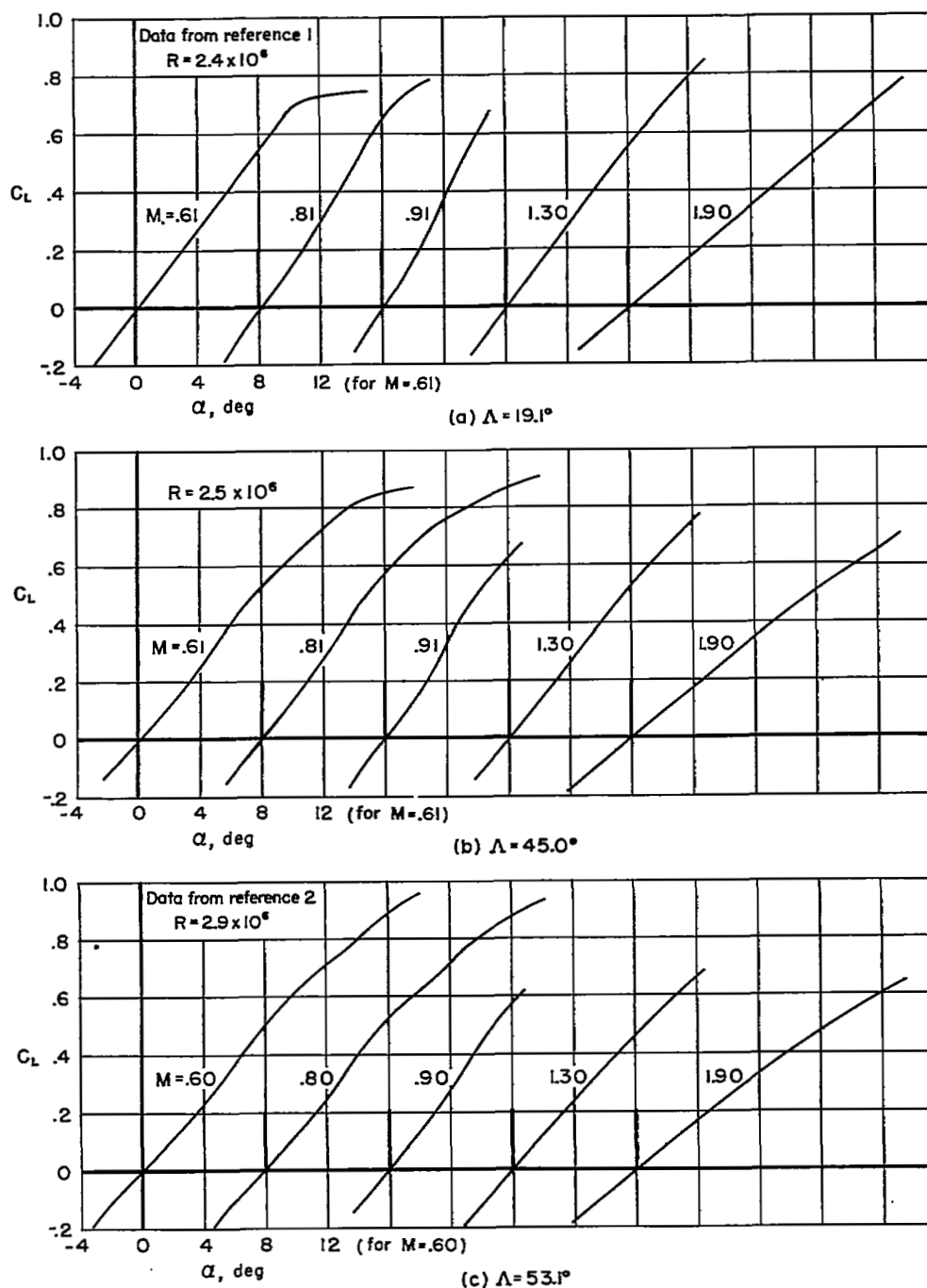


Figure 5.- Variation of lift coefficient with angle of attack for wings having  $19.1^\circ$ ,  $45.0^\circ$ , and  $53.1^\circ$  sweepback of the leading edge.

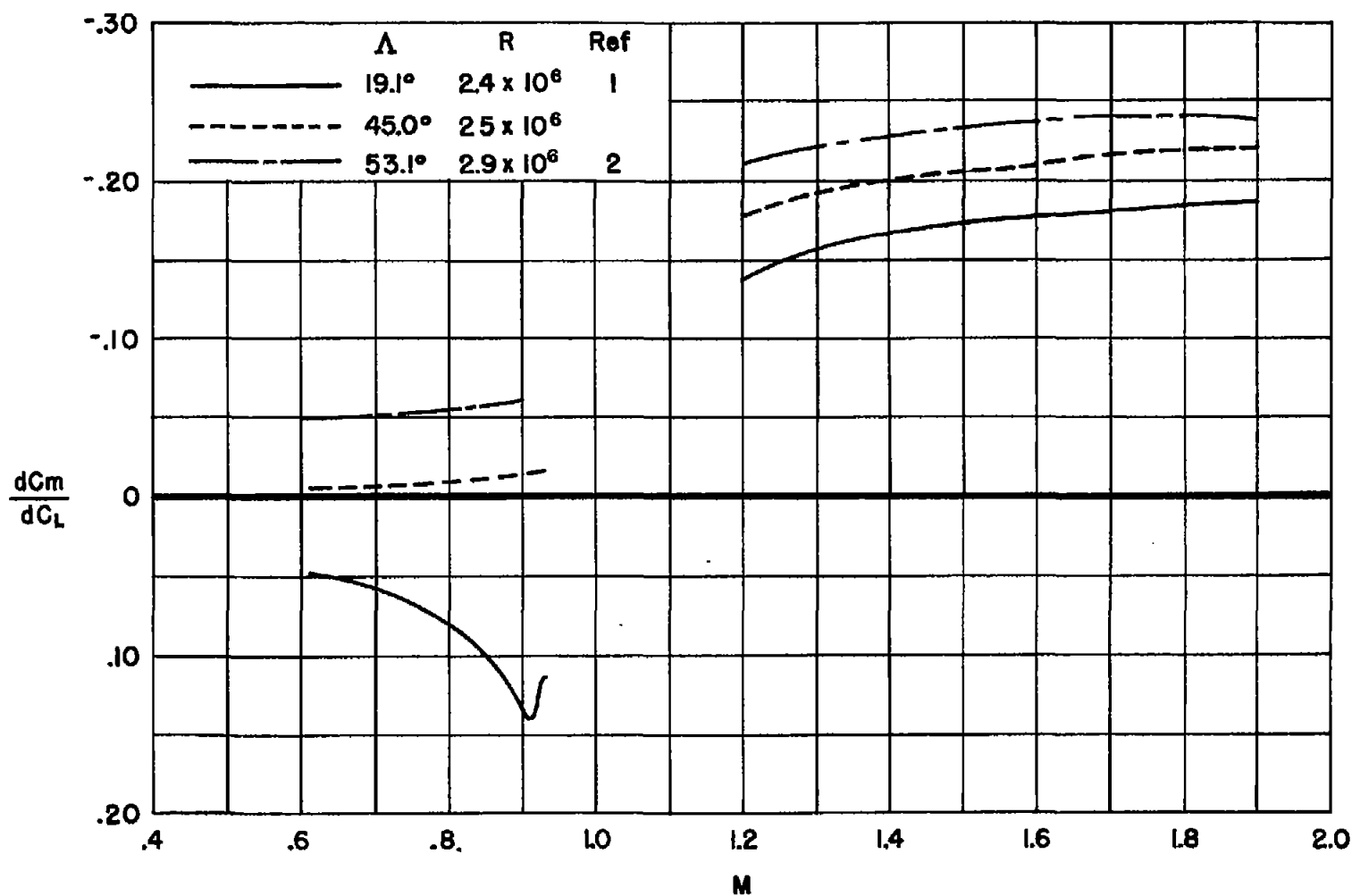


Figure 6.- Effect of leading-edge sweepback on the variation with Mach number of the experimental static longitudinal stability derivative measured at zero lift.

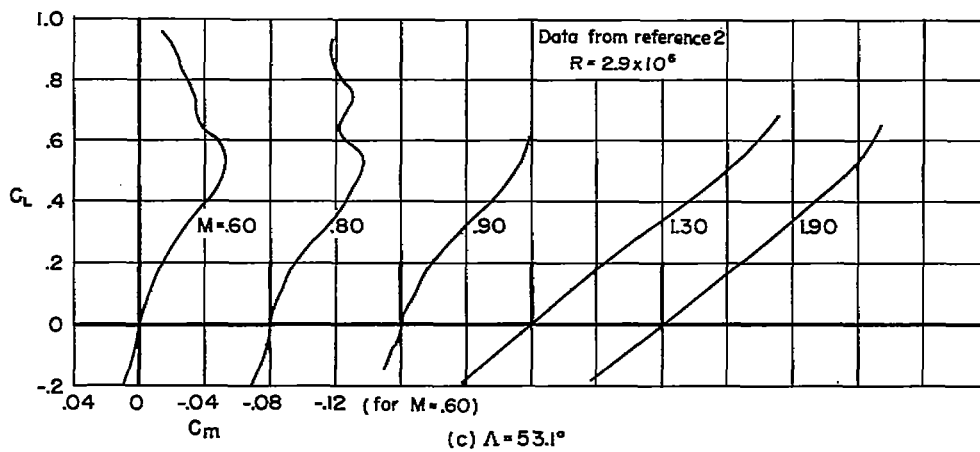
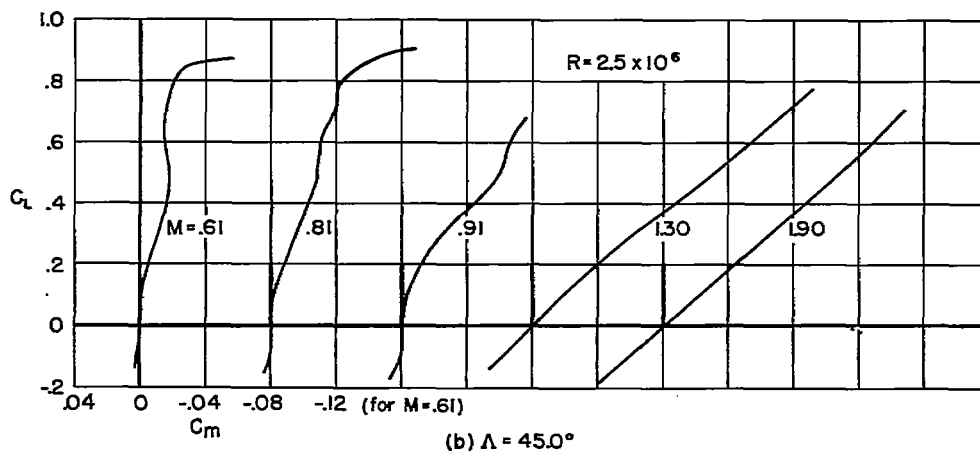
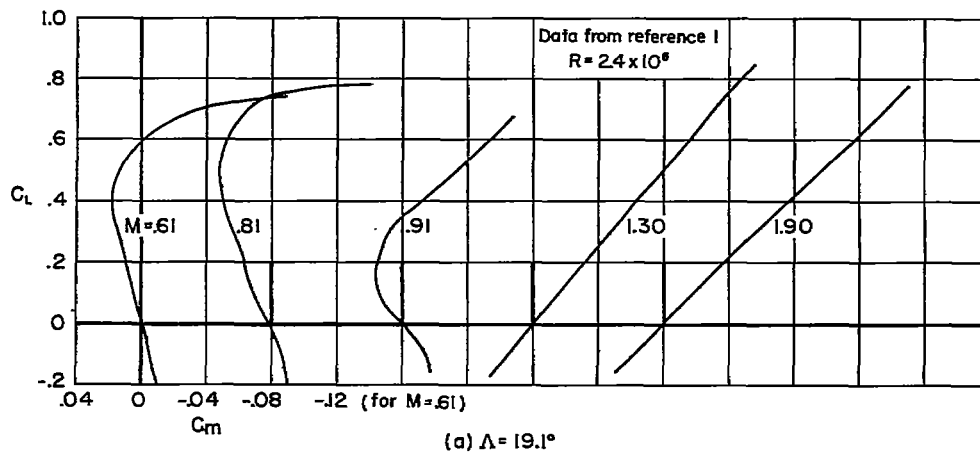


Figure 7.- Variation of pitching-moment coefficient with lift coefficient for wings having  $19.1^\circ$ ,  $45.0^\circ$ , and  $53.1^\circ$  sweepback of the leading edge.

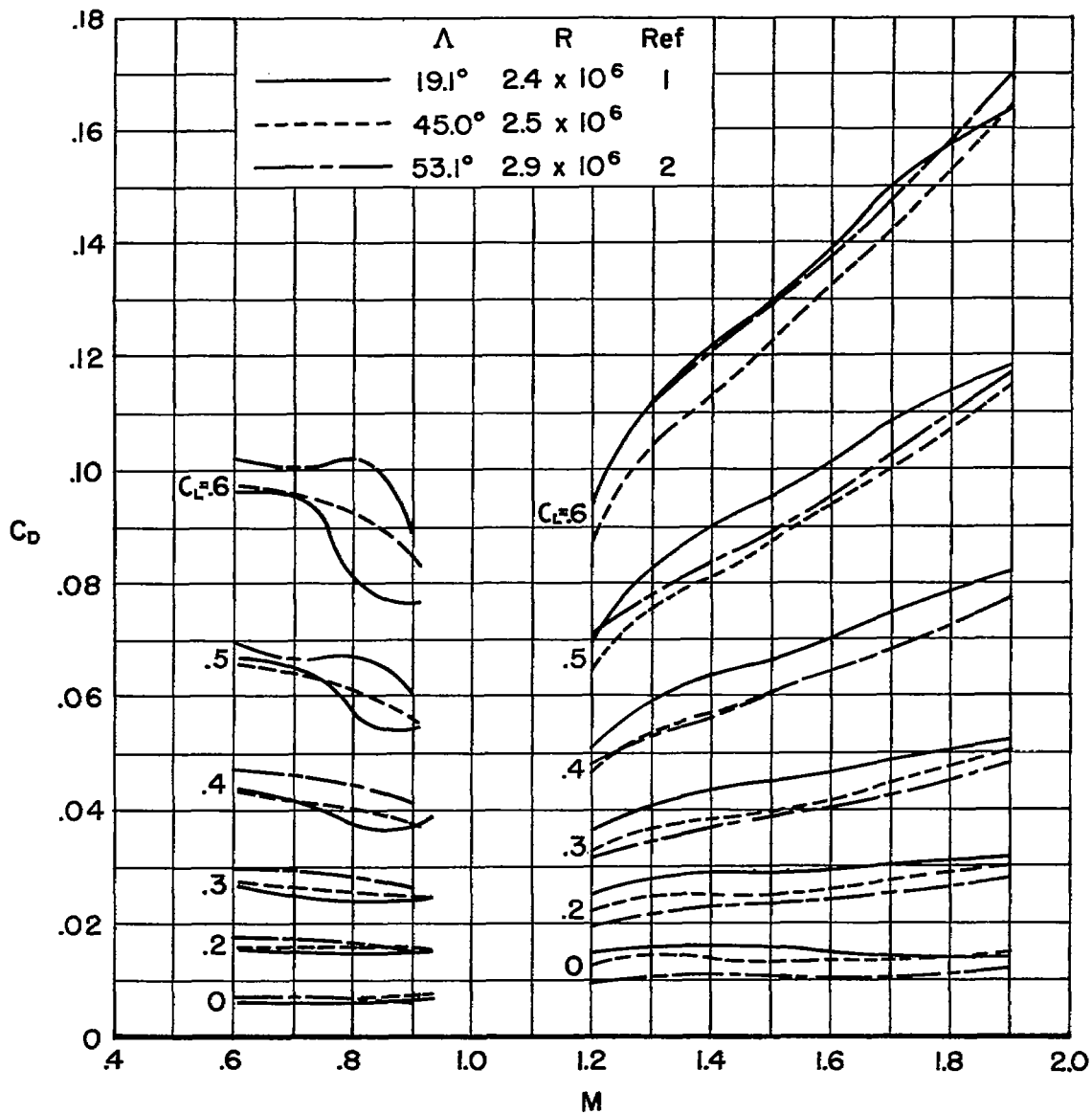


Figure 8.- Effect of leading-edge sweepback on the variation with Mach number of the drag coefficient measured at various lift coefficients.

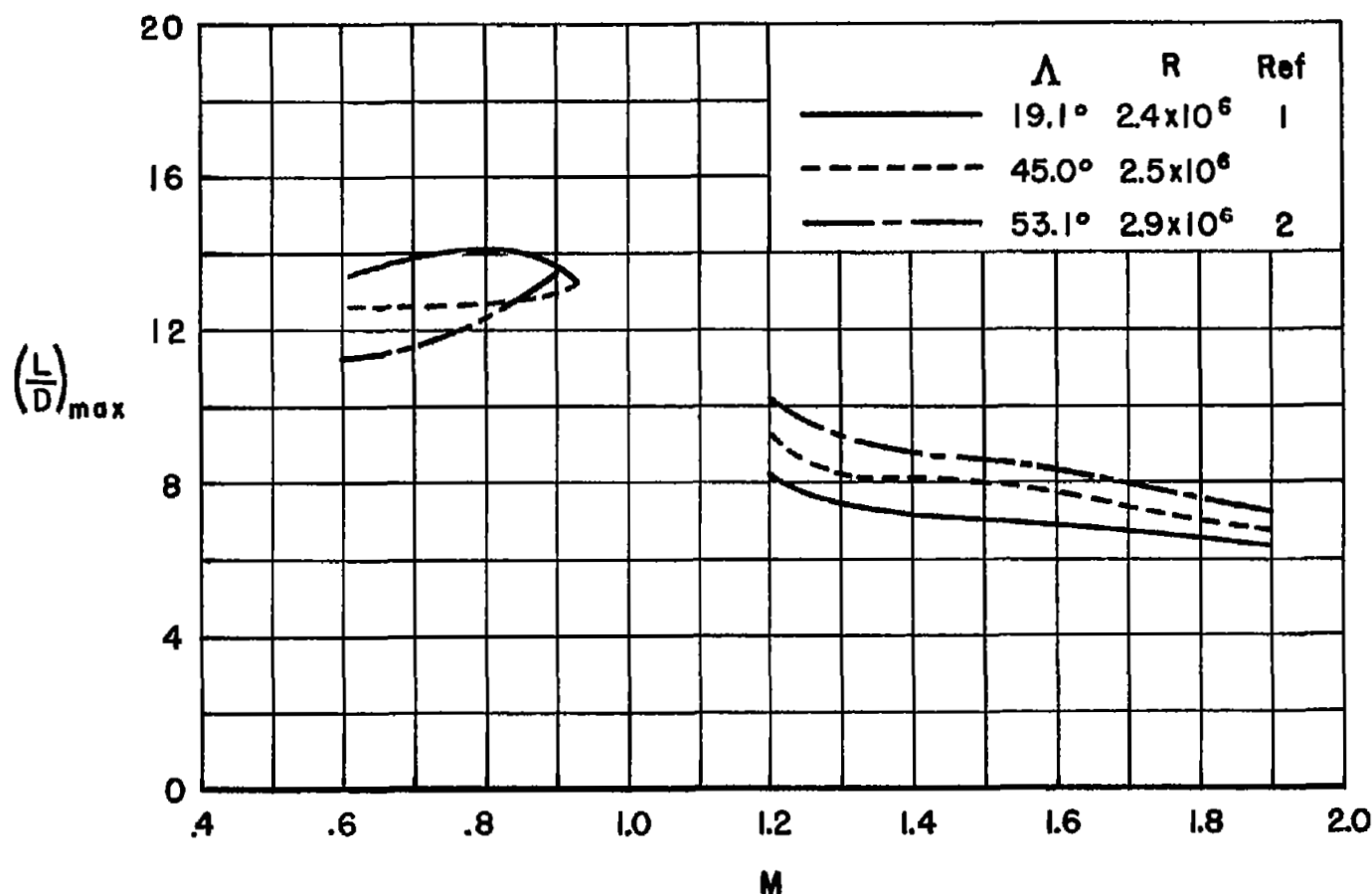
(a)  $(L/D)_{\max}$  vs.  $M$ 

Figure 9.- Effect of leading-edge sweepback on the variation with Mach number of the maximum lift-drag ratio and the range parameter  $M(L/D)_{\max}$ .

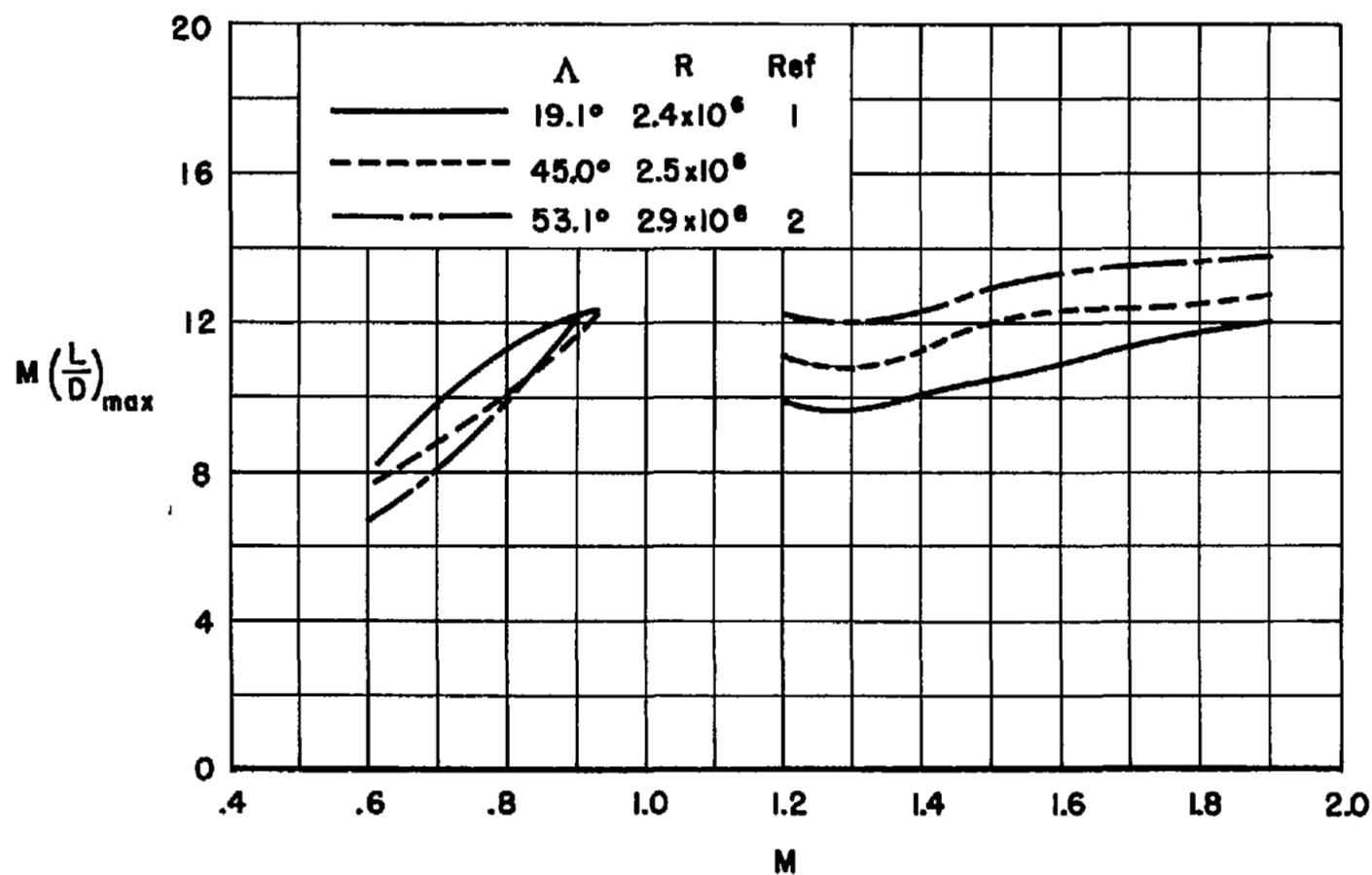
(b)  $M(L/D)_{\max}$  vs.  $M$ 

Figure 9.- Concluded

~~CONFIDENTIAL~~



3 1176 01434 8602

~~CONFIDENTIAL~~